Direction-of-Arrival Tracking of Multiple Fast-Moving Sources in Antenna Array based Access Networks

Zhuqing Tang and Athanassios Manikas
Department of Electrical and Electronics Engineering
Imperial College London

***Abstract*—This paper is concerned with the problem of simultaneously tracking the direction-of-arrival (DOA) of multiple fast moving sources using the vector-signal received by a small aperture antenna array of N elements. The antenna array may be located at the Node-B, eNode-B or gNode-B of an access network and is used in conjunction with a novel trajectory tracking algorithm. The proposed algorithm incorporates a "manifold extender" together with a state space model and an arrayed extended Kalman filter (EKF). These provide a spatiotemporal tracking approach of the DOAs and angular velocities of multiple fast moving sources snapshot-by-snapshot. Furthermore, two different manifold extenders are employed in the proposed algorithm and their performance is evaluated using computer simulation studies and is compared with the case where the proposed algorithm is implemented without a "manifold extender".**

***Index Terms*—Array signal processing, source tracking, extended Kalman filter, spatiotemporal, direction-of-arrival, array manifolds, extended manifolds**

NOTATION

$A,\ a$	Scalar
$\underline{A},\ \underline{a}$	Column vector
$\mathbb{A}, \mathbf{A}, \mathbf{r}$	Matrix
$(\cdot)^T$	Transpose
$(\cdot)^H$	Hermitian transpose
$\mathcal{E}\{\cdot\}$	Expectation operator
$\mathbb{I}_N$	$N \times N$ Identity matrix
$\underline{1}_N$	Column vector of N ones
$\mathcal{R}$	Set of real numbers
$\mathcal{C}$	Set of complex numbers
$\exp(\underline{A})$	Element by element exponential of vector $\underline{A}$
∇	Vector differential operator

I. INTRODUCTION

Tracking the direction-of-arrival (DOA) of multiple moving sources/users[1] is a significant research topic in array signal processing, due to its wide applications in sonar, radar, air traffic control, mobile communications, remote sensing, etc. For static sources, it is well known that their DOA can be estimated using, for instance, signal-subspace algorithms (e.g. [1], [2], [3]). If the motion of the sources is slow, then small time-frames can be used and, for each time-frame, apply a DOA estimation algorithm (i.e. repetitive DOA estimation) tracking small variations in DOA.

However, if the source is moving too fast so that the source cannot be assumed stationary over a small time-frame, these high-resolution algorithms with repetitive DOA estimation begin to exhibit performance degradation. Thus, various iterative DOA algorithms have been proposed which however suffer from the data association problem. Several approaches ([4]-[8]) have been proposed to avoid this problem by maintaining the order of the DOA estimates for different iterations. However, these approaches suffer from spread array spatial spectrum effects caused by rapid source motion [9].

To remedy the aforementioned problems, various algorithms based on state space models have been proposed. For example, a maximum likelihood (ML) approach combined with a multiple target state model has been proposed in [9]. In [10], a Bayesian model is utilised in conjunction with a particle filter to track the targets. However, these approaches have high computational complexity. In [11], a linear combiner matrix is constructed as a state variable, which is updated adaptively by an H-infinity filter, to obtain the adaptive estimated noise subspaces for tracking the DOAs.

Another widely adopted family of algorithm for source tracking is based on the Kalman filter (KF) which recursively tracks source parameters snapshot-by-snapshot with the use of a state space model. It has less computational complexity and been used in communication systems, e.g. [12]. However, KF cannot handle nonlinear estimation problems which can be solved by an extended Kalman filter (EKF), e.g. [13]-[15]. The proposed algorithm presented in this paper belongs to the EKF family of algorithm.

In particular, to track the DOA of multiple fast-moving sources, a novel tracking approach is proposed using a small aperture antenna array of N elements and a spatiotemporal state space model integrated with an arrayed EKF algorithm. This approach utilises a "manifold extender" to increase the signal observation space from N to $N\mathcal{N}_{\text{ext}}$ (where $\mathcal{N}_{\text{ext}}$ is a positive integer) and to construct ($N\mathcal{N}_{\text{ext}} \times 1$) extended manifold vectors. Then, the spatiotemporal state space model incorporates these extended manifold vectors to track the

[1]In this paper, the terms "sources", "users", and "emitters" are considered equivalent and may be used interchangeably.

DOAs of the sources snapshot-by-snapshot.

The remainder of this paper is organised as follows. In Section II, the array system is presented and the received extended signal vector is modelled. In Section III, the mobility model of the multiple sources is described. Based on this, the proposed spatiotemporal state space model is constructed, and then it is combined with an arrayed EKF in Section IV. In Section V, the proposed approach is evaluated using computer simulation studies. Finally, this paper is concluded in Section VI.

II. Array System Model

Consider a Node-B, eNode-B or gNode-B that employs an array system of N antennas operating in the presence of M sources. Each source transmits a data sequence $\{\mathrm{a}[n]\}$ that is weighted by a PN-code of length $\mathcal{N}_c$. That is, for the i-th source shown in Figure 1, the transmitted data sequence at point-A is $\{\mathrm{a}_i[n]\}$ (with data symbol period T_{cs}) with each symbol weighted by the $\mathcal{N}_c \times 1$ weight-code vector

$$\underline{w}_i \triangleq [w_i[1], w_i[2], ..., w_i[q], ..., w_i[\mathcal{N}_c]]^T \tag{1}$$

with

$$w_i[q] \in \pm 1, q \in [1, \mathcal{N}_c] \tag{2}$$

and

$$\underline{w}_i^T \underline{w}_j \simeq \begin{cases} 1, & \text{for } i = j \\ 0, & \text{for } i \neq j \end{cases} \tag{3}$$

Then, each weighted data symbol is driven to a Digital-to-Analogue Converter (DAC) that produces at point-C (see Figure 1) a baseband transmitted signal $m_i(t)$.

At the receiver, consider a fully calibrated array of N antennas whose locations are given by

$$\mathbf{r} = [\underline{r}_1, \underline{r}_2, ..., \underline{r}_m ..., \underline{r}_N] \in \mathcal{R}^{3\times N} \tag{4}$$

where the vector $\underline{r}_m \in \mathcal{R}^{3\times 1}$ denotes the Cartesian coordinates of the m-th array element.

As the array operates in the presence of M narrowband far-field sources/users, the $(N \times 1)$ received baseband vector signal $\underline{x}(t)$ at point-D can be modelled as follows

$$\underline{x}(t) = \sum_{i=1}^{M} \beta_i(t) \exp(j2\pi \mathcal{F}_i t) \underline{S}_i(t) m_i(t) + \underline{\mathrm{n}}(t) \tag{5}$$

where, for the i-th source, $\beta_i(t)$ denotes the time varying path fading coefficient, $\mathcal{F}_i$ represents the Doppler frequency and the vector $\underline{\mathrm{n}}(t)$ denotes the additive white Gaussian noise of zero mean and covariance matrix given by

$$\mathbb{R}_{\mathrm{nn}} = \sigma_{\mathrm{n}}^2 \mathbb{I}_N \tag{6}$$

with σ_{n}^2 representing the noise power.

In Eq. (5), $\underline{S}_i(t) \in \mathcal{C}^{N\times 1}$ denotes the time-varying manifold vector which is given as follows

$$\underline{S}_i(t) = \exp\left(-j\frac{2\pi F_c}{c}\mathbf{r}^T \underline{u}_i(t)\right) \tag{7}$$

where F_c is the carrier frequency, c is the velocity of light and $\underline{u}_i(t)$ is given by

$$\underline{u}_i(t) = \begin{bmatrix} \cos\theta_i(t)\cos\phi_i(t) \\ \sin\theta_i(t)\cos\phi_i(t) \\ \sin\phi_i(t) \end{bmatrix} \tag{8}$$

with $\theta_i(t)$ and $\phi_i(t)$ representing the azimuth and the elevation angles of the i-th source. In this paper, with no loss

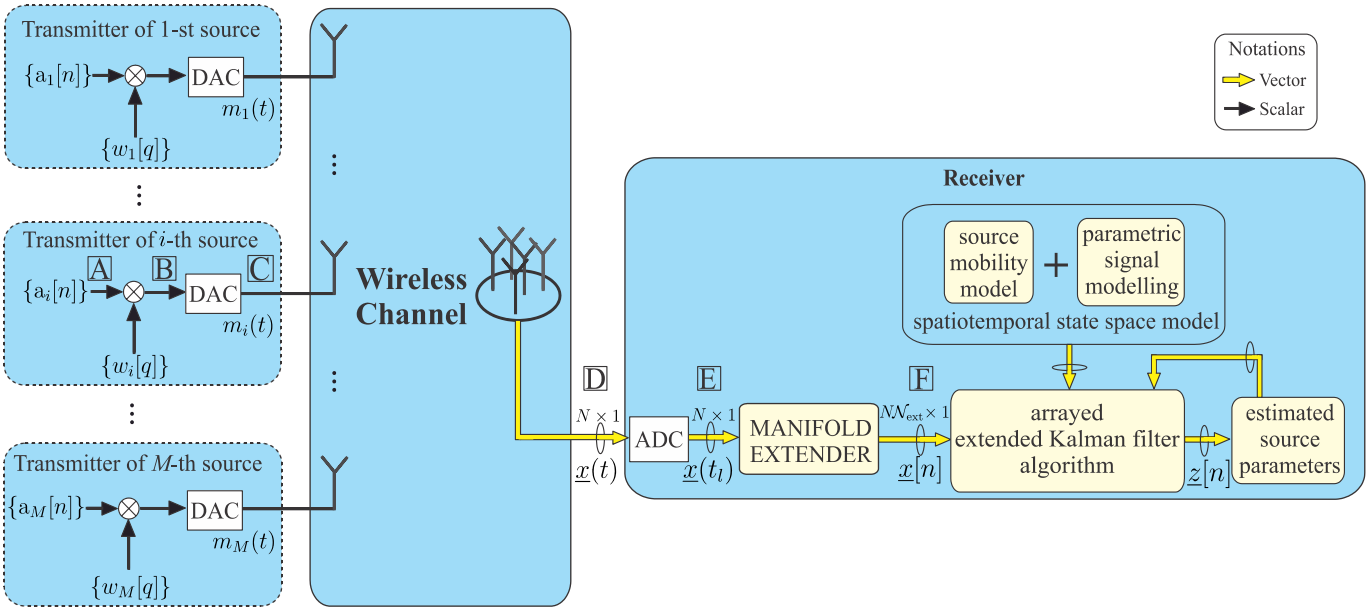


Figure 1. Baseband representation of the array system model consisting of M transmitters (Tx), a SIMO multiuser wireless channel and an array receiver.

of generality, the elevation angle is assumed to be zero (i.e. $\phi_i(t) = 0$).

Eq. (5) can also be written in a more compact form as follows

$$\underline{x}(t) = \mathbb{S}(t)\underline{m}(t) + \underline{\mathrm{n}}(t) \tag{9}$$

where

$$\mathbb{S}(t) = [\underline{S}_1(t), ..., \underline{S}_i(t), \ldots, \underline{S}_M(t)] \in \mathcal{C}^{N\times M} \tag{10}$$

and

$$\underline{m}(t) = \begin{bmatrix} \beta_1(t)\exp(j2\pi\mathcal{F}_1 t)m_1(t) \\ \beta_2(t)\exp(j2\pi\mathcal{F}_2 t)m_2(t) \\ \vdots \\ \beta_M(t)\exp(j2\pi\mathcal{F}_M t)m_M(t) \end{bmatrix} \in \mathcal{C}^{M\times 1} \tag{11}$$

with its covariance matrix $\mathbb{R}_{mm}$ given as

$$\mathbb{R}_{mm} = \mathcal{E}\left\{(\underline{m}(t) - \mathcal{E}\{\underline{m}(t)\})(\underline{m}(t) - \mathcal{E}\{\underline{m}(t)\})^H\right\} \tag{12}$$

The $(N \times 1)$ vector signal $\underline{x}(t)$ in Eq. (9) is then discretised and, at point-F, the $(N\mathcal{N}_{\text{ext}} \times 1)$ vector signal $\underline{x}[n]$ can be expressed as follows

$$\underline{x}[n] = \mathbb{H}[n]\,\underline{m}[n] + \underline{\mathrm{n}}[n] \tag{13}$$

where the matrix $\mathbb{H}[n] \in \mathcal{C}^{N\mathcal{N}_{\text{ext}}\times M}$ is given by

$$\mathbb{H}[n] = [\underline{h}_1[n], ..., \underline{h}_i[n], \ldots, \underline{h}_M[n]] \tag{14}$$

with $\underline{h}_i[n] \in \mathcal{C}^{N\mathcal{N}_{\text{ext}}\times 1}$ representing the time-varying extended manifold vector of the i-th source given as follows

$$\underline{h}_i[n] = \underline{S}_i[n] \otimes \underline{w}_i \tag{15}$$

In addition, the vector $\underline{\mathrm{n}}[n] \in \mathcal{C}^{N\mathcal{N}_{\text{ext}}\times 1}$ denotes the discretised extended noise, at point-F in Figure 1, and $\mathcal{N}_{\text{ext}} = \mathcal{N}_c$.

It is important to point out that if the source to be tracked does not include the weight $\underline{w}_i$, then this corresponds to $\underline{w}_i = \underline{1}_{\mathcal{N}_c}$, and the extended manifold vector of Eq. (15) is simplified to

$$\underline{h}_i[n] = \underline{S}_i[n] \otimes \underline{1}_{\mathcal{N}_c} \tag{16}$$

That is, the extended manifold vector in Eq. (14) can be expressed as

$$\underline{h}_i[n] = \begin{cases} \underline{S}_i[n] \otimes \underline{w}_i & \text{with PN-code weight at Tx} \\ \underline{S}_i[n] \otimes \underline{1}_{\mathcal{N}_c} & \text{without PN-code weight at Tx} \end{cases} \tag{17}$$

III. Multi-source mobility model

The mobility model of the i-th source, for $i = 1, 2, ..., M$, is shown in Figure 2 relative to the array reference point. Figure 2 shows that the i-th source moves in a particular direction with velocity vector $\underline{v}_i \in \mathcal{R}^{3\times 1}$ given as follows

$$\underline{v}_i = v_{\rho_i}\underline{u}_{v_{\rho_i}} + v_{\theta_i}\underline{u}_{v_{\theta_i}} \tag{18}$$

where the velocity vector $\underline{v}_i$ is decomposed into two other vectors:

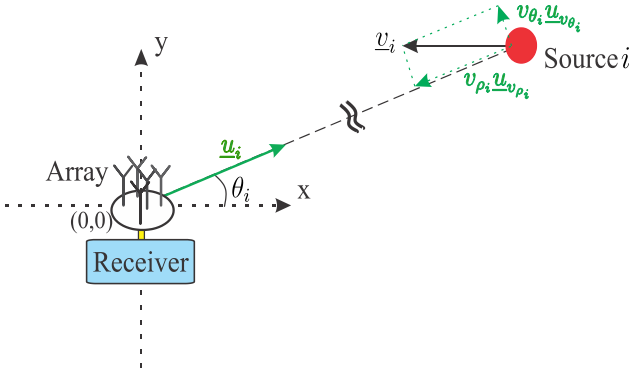


Figure 2. Illustration of the mobility model of the i-th source/user. The velocity vector $\underline{v}_i$ of the source is decomposed into its radial term $v_{\rho_i}\underline{u}_{v_{\rho_i}}$ and the orthoradial term $v_{\theta_i}\underline{u}_{v_{\theta_i}}$, respectively. The sign of the unit vectors $\underline{u}_{v_{\rho_i}}$ and $\underline{u}_{v_{\theta_i}}$ can be either positive or negative. The direction θ_i of the source is measured with respect to the array reference point.

- the radial component $v_{\rho_i}\underline{u}_{v_{\rho_i}}$, and
- the orthoradial (i.e. angular) component $v_{\theta_i}\underline{u}_{v_{\theta_i}}$,

with v_{ρ_i} denoting the radial velocity of the i-th source and v_{θ_i} representing its azimuthal velocity. The vectors $\underline{u}_{v_{\rho_i}}$ and $\underline{u}_{v_{\theta_i}}$ are unity norm vectors and they are orthogonal to each other. The radial velocity v_{ρ_i} causes the Doppler frequency effects but only the azimuthal velocity v_{θ_i} affects the direction-of-arrival θ_i. Thus, if the i-th source moves with a constant azimuthal velocity, its azimuth angle may be described as

$$\theta_i(t) = \theta_i(t_0) + v_{\theta_i}(t_0)\,T \tag{19}$$

where

$$T = t - t_0 \tag{20}$$

is the time elapsed between t and t_0. If T is assumed to be equal to the sampling period, i.e.

$$\begin{aligned} t_0 &= (n-1)T \\ t &= nT \end{aligned}$$

then Eq. (19) is discretised and becomes

$$\theta_i[n] = \theta_i[n-1] + v_{\theta_i}[n]T \tag{21}$$

Consequently, if we define the discrete-time state vector for the i-th source as $\underline{z}_i[n]$, i.e.

$$\underline{z}_i[n] \triangleq \begin{bmatrix} \theta_i[n] \\ v_{\theta_i}[n] \end{bmatrix} \tag{22}$$

then the discrete time *kinematic model* for the i-th source for $t = nT$ is given as

$$\underline{z}_i[n] = \mathbb{F}_i\underline{z}_i[n-1] + \underline{\tilde{z}}_i[n] \tag{23}$$

where $\mathbb{F}_i \in \mathcal{R}^{2\times 2}$ is the state transition matrix given by

$$\mathbb{F}_i = \begin{bmatrix} 1 & T \\ 0 & 1 \end{bmatrix} \tag{24}$$

In Eq. (23), $\widetilde{\underline{z}}_i[n] \in \mathcal{R}^{2\times 1}$ represents perturbations about the azimuth angle and the azimuthal velocity, and can be modelled as "noise" with zero mean and covariance matrix $\mathbb{Q}_i \in \mathcal{R}^{2\times 2}$ given by

$$\mathbb{Q}_i = \sigma^2_{\theta_i} \left[\begin{array}{cc} \frac{T^3}{3}, & \frac{T^2}{2} \\ \frac{T^2}{2}, & T \end{array} \right] \tag{25}$$

where $\sigma^2_{\theta_i}$ denotes the continuous time model intensity for the azimuth-velocity. Then, the discrete time multi-source kinematic model of all the M sources can be expressed as a generalisation of Eq. (23) as follows

$$\underline{z}[n] = \mathbb{F}\underline{z}[n-1] + \widetilde{\underline{z}}[n] \tag{26}$$

where

$$\underline{z}[n] = \left[\underline{z}_1^T[n], \underline{z}_2^T[n], \ldots, \underline{z}_M^T[n]\right]^T \in \mathcal{R}^{2M\times 1} \tag{27}$$

$$\widetilde{\underline{z}}[n] = \left[\widetilde{\underline{z}}_1^T[n], \widetilde{\underline{z}}_2^T[n], \ldots, \widetilde{\underline{z}}_M^T[n]\right]^T \in \mathcal{R}^{2M\times 1} \tag{28}$$

$$\mathbb{F} = \mathbb{I}_M \otimes \mathbb{F}_i \in \mathcal{R}^{2M\times 2M} \tag{29}$$

Based on the above, the covariance matrix $\mathbb{P}[n] \in \mathcal{R}^{2M\times 2M}$ of the discrete time state vector $\underline{z}[n]$ is

$$\mathbb{P}[n] = \mathbb{F}\mathbb{P}[n-1]\mathbb{F}^T + \mathbb{Q} \tag{30}$$

where the matrix $\mathbb{Q} \in \mathcal{R}^{2M\times 2M}$ is a block diagonal matrix containing the individual covariances $\mathbb{Q}_i$ of all sources.

IV. Tracking using Spatiotemporal state space model

In this section, the proposed tracking algorithm is presented which employs a state space model that is based on the parametric modelling of the received antenna array signal and the mobility model presented in the previous section. In particular, based on the extended snapshot in Eq. (13) and the state vector in Eq. (26), this state space model is constructed as follows

$$\underline{z}\,[n] = \mathbb{F}\underline{z}\,[n-1] + \widetilde{\underline{z}}\,[n] \tag{31}$$

$$\underline{x}\,[n] = \mathbb{H}\left(\underline{z}\,[n]\right)\underline{m}\,[n] + \underline{\mathrm{n}}\,[n] \tag{32}$$

describing the dynamics of the source motion and the vector signal received by the array.

The proposed tracking algorithm is summarised in Table I using a simplified notation by redefining the following parameters

$$\begin{aligned} \underline{z}_n \triangleq \underline{z}\,[n] &\in \mathcal{R}^{2M\times 1} \\ \mathbb{P}_n \triangleq \mathbb{P}[n] &\in \mathcal{R}^{2M\times 2M} \\ \underline{x}_n \triangleq \underline{x}\,[n] &\in \mathcal{C}^{N\mathcal{N}_{\mathrm{ext}}\times 1} \\ \underline{m}_n \triangleq \underline{m}\,[n] &\in \mathcal{C}^{M\times 1} \end{aligned}$$

With reference to Table I, the initial state $\underline{z}_0$ can be provided by a priori guess and the initial covariance $\mathbb{P}_0$ can be set to $\lambda\mathbb{I}_{2M}$ where λ indicates the confidence level in the accuracy of the initial estimates.

TABLE I
THE ARRAYED EXTENDED KALMAN FILTER TRACKING ALGORITHM

Tracking Algorithm based on Arrayed-EKF
Initialisation
$\widehat{\underline{z}}_0 = \mathcal{E}\left\{\underline{z}_0\right\}$
$\mathbb{P}_0 = \mathcal{E}\left\{\left(\underline{z}_0 - \widehat{\underline{z}}_0\right)\left(\underline{z}_0 - \widehat{\underline{z}}_0\right)^T\right\} = \lambda\mathbb{I}_{2M}$
for n = 1,2,3...
A Priori Estimation of States
$\widehat{\underline{z}}_n = \mathbb{F}\widehat{\underline{z}}_{n-1}$
$\mathbb{P}_n = \mathbb{F}\mathbb{P}_{n-1}\mathbb{F}^T + \mathbb{Q}$
Estimation of the Transmitter Baseband Signals
$\widehat{\underline{m}}_n = \mathbb{R}_{mm}\mathbb{H}^H(\widehat{\underline{z}}_n)\left(\sigma^2_{\mathrm{n}}\mathbb{I}_{N\mathcal{N}_{\mathrm{ext}}} + \mathbb{H}(\widehat{\underline{z}}_n)\mathbb{R}_{mm}\mathbb{H}^H(\widehat{\underline{z}}_n)\right)^{-1}\underline{x}_n$
A Posteriori Estimation of States
$\mathbb{D}_n = \nabla_{\underline{z}_n}\left(\mathbb{H}\left(\underline{z}_n\right)\widehat{\underline{m}}_n\right)_{\underline{z}_n = \widehat{\underline{z}}_n}$
$\mathbb{K}_n = \mathbb{P}_n\mathbb{D}_n^H\left(\mathbb{D}_n\mathbb{P}_n\mathbb{D}_n^H + \sigma^2_{\mathrm{n}}\mathbb{I}_{N\mathcal{N}_{\mathrm{ext}}}\right)^{-1}$
$\widehat{\underline{z}}_n = \widehat{\underline{z}}_n + \mathrm{Re}\left\{\mathbb{K}_n\left(\underline{x}_n - \mathbb{H}(\widehat{\underline{z}}_n)\widehat{\underline{m}}_n\right)\right\}$
$\mathbb{P}_n = \left(\mathbb{I}_{2M} - \mathbb{K}_n\mathbb{D}_n\right)\mathbb{P}_n$
end

In addition, please note that the extended manifold vector in this model has two forms/cases as described in Eq. (17) and the proposed algorithm can be applied for both cases using a manifold extender with $\mathcal{N}_{\mathrm{ext}} = \mathcal{N}_c$. However, the proposed algorithm shown in Table I also can be used for the case that the manifold extender is not used. In this case, $\mathcal{N}_{\mathrm{ext}} = 1$ and $\mathbb{H}\,[n] = \mathbb{S}\,[n]$, which implies that the i-th column of $\mathbb{H}\,[n]$ is $\underline{h}_i[n] = \underline{S}_i[n]$. Thus, Eq. (17) can be upgraded to include the absence of the "manifold extender" as follows

$$\underline{h}_i\,[n] = \left\{ \begin{array}{lll} \underline{S}_i\,[n] \otimes \underline{w}_i & \in \mathcal{C}^{N\mathcal{N}_{\mathrm{ext}}\times 1}; & \text{case-1} \\ \underline{S}_i\,[n] \otimes \underline{1}_{\mathcal{N}_{\mathrm{ext}}} & \in \mathcal{C}^{N\mathcal{N}_{\mathrm{ext}}\times 1}; & \text{case-2} \\ \underline{S}_i\,[n] & \in \mathcal{C}^{N\times 1}; & \text{case-3} \end{array} \right| \tag{33}$$

V. Computer simulation studies

The performance of the proposed approach is evaluated in this section using computer simulation studies. The antenna array at the base station is assumed (without any loss of generality) to be a grid planar array of 9 elements as this is

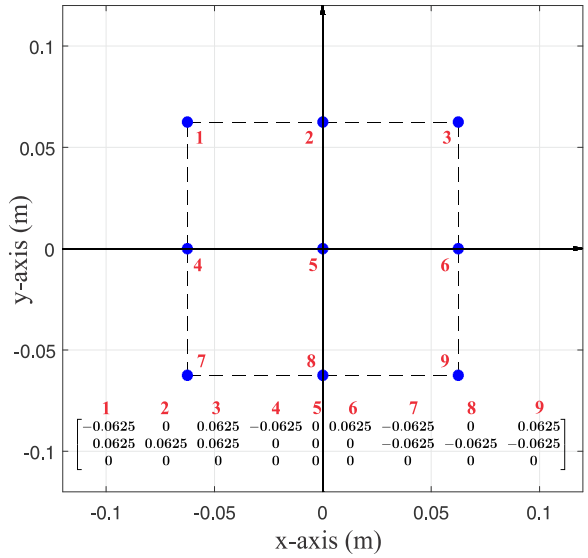


Figure 3. The grid planar array of $N = 9$ antennas, used in Section V, and their Cartesian coordinates.

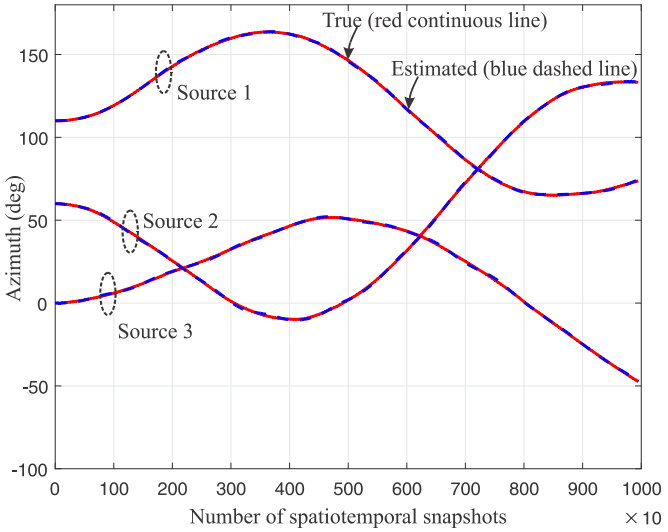


Figure 4. Case-1: true (red line) and estimated (blue dashed line) azimuth trajectories using the extended manifold vector $\underline{h}_i[n] = \underline{S}_i[n] \otimes \underline{w}_i$. (SNR = 10 dB)

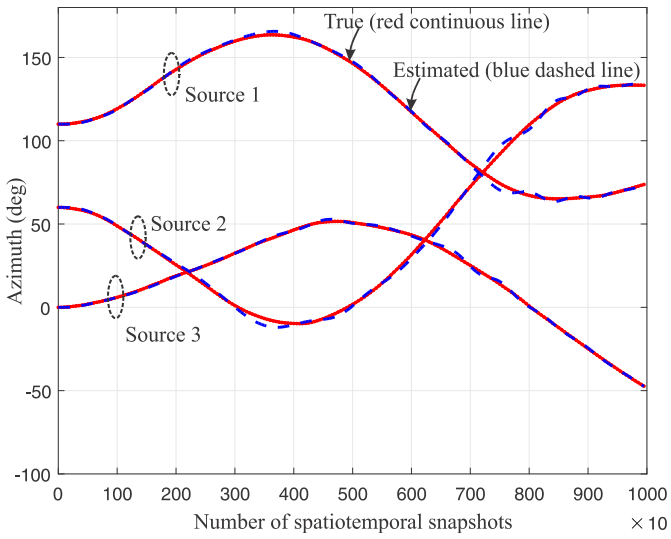


Figure 5. Case-2: true (red line) and estimated (blue dashed line) azimuth trajectories using the extended manifold vector $\underline{h}_i[n] = \underline{S}_i[n] \otimes \underline{1}_{\mathcal{N}_{\text{ext}}}$. (SNR = 10 dB)

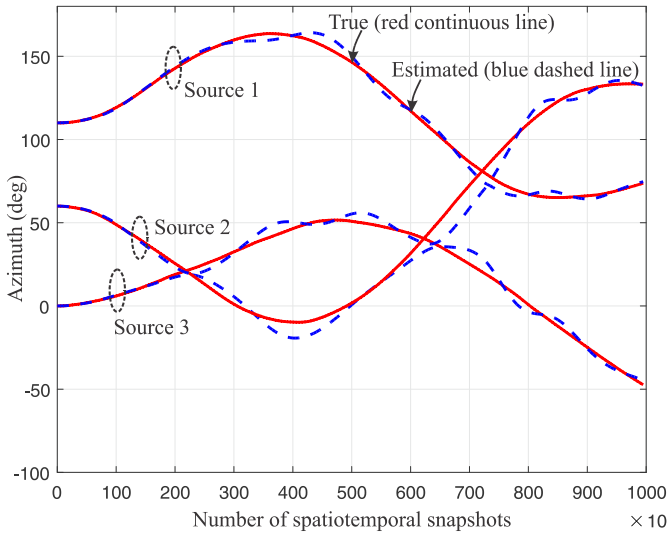


Figure 6. Case-3: true (red line) and estimated (blue dashed line) azimuth trajectories using the spatial manifold vector $\underline{h}_i[n] = \underline{S}_i[n]$. (SNR = 10 dB)

shown in Figure 3. Furthermore, it is assumed that the array operates in the presence of 3 far-field moving sources/users transmitting at the same time on the same frequency band and their initial azimuthal velocities are assumed to be $0°/T$.

The data sequence transmitted by each source/user is assumed to be a random sequence of ± 1s of zero mean and unity variance. The weight-code vectors are gold codes and the length $\mathcal{N}_c$ is set to 15. The carrier frequency is set to 2.4 GHz. The source tracking is assumed to be carried out over a time interval of 10000 spatiotemporal snapshots $\underline{x}[n] \in \mathcal{C}^{N\mathcal{N}_c \times 1}$. The continuous time model intensity for the azimuth-velocity (see Eq. (25)) is set to $\sigma^2_{\dot{\theta}_i} = 10^{-8}(\text{deg}/T)^2, \forall i$. The parameter λ of the initialisation stage of the proposed algorithm (see Table I) is set to 10^{-6}.

Figure 4 shows the estimated DOA (azimuth) trajectories of the three moving sources using the proposed approach for the first case in Eq. (33), i.e. for $\underline{h}_i[n] = \underline{S}_i[n] \otimes \underline{w}_i$, assuming that SNR = 10 dB. It is clear that the proposed algorithm tracks the DOAs with high accuracy.

Furthermore, Figures 5 and 6 illustrate the tracking capabilities of the proposed approach for the case-2 and the case-3 in Eq. (33), under the same simulation environment. Similar results can be obtained if the SNR is reduced to 0 dB and Figure 7 shows the results of SNR = 0 dB for the case-1, as a representative result.

Finally, the performance of the proposed approach for all the three cases of Eq. (33) is examined using Monte-Carlo computer simulation studies. The results are shown in Figure 8

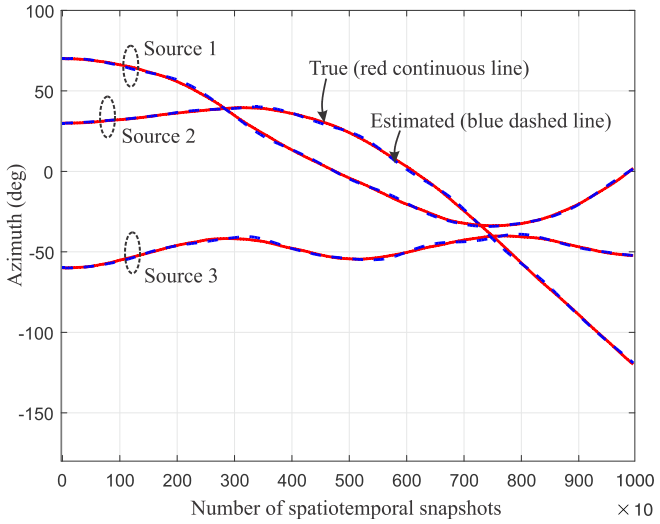


Figure 7. Case-1: true (red line) and estimated (blue dashed line) azimuth trajectories for SNR = 0 dB.

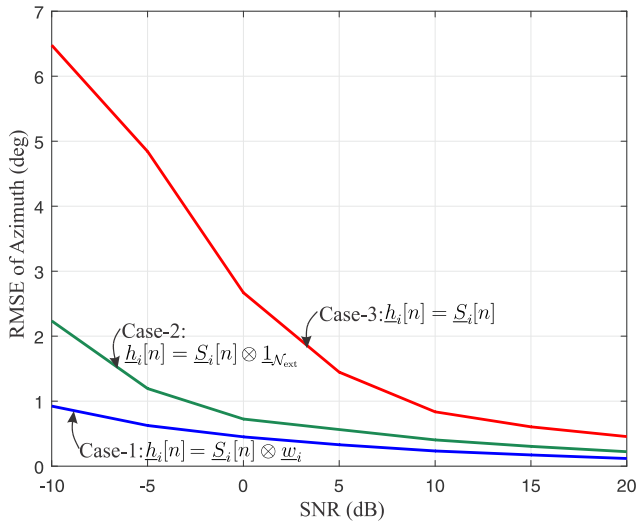


Figure 8. RMSE of the estimated source azimuth angles averaged over 5000 spatiotemporal snapshots using the proposed approach for the three cases as a function of the SNR (100 iterations).

where the root mean square error (RMSE) of the estimated azimuth angles (averaged over 5000 spatiotemporal snapshots) is plotted as a function of the SNR. It is evident in Figure 8 that the case-1 of the proposed approach has better source tracking performance over the whole SNR range than the case-2 and the case-3.

By observing the results when the SNR is low (i.e. SNR = -10 dB), it is clear that the case-1 is the most robust to noise effects, followed by the case-2, and then by the case-3. This is because the "manifold extender" increases the degrees-of-freedom by increasing the dimensionality of the observation space of the data from N to $N\mathcal{N}_{\text{ext}}$ where $\mathcal{N}_{\text{ext}}$ is a positive integer.

If there is no manifold extender, then $\mathcal{N}_{\text{ext}} = 1$, and to increase the dimensionality of the observation space we need to increase the number of antenna elements N. However, this implies more hardware resources and consequently, higher cost.

VI. Conclusions

In this paper, a novel approach was proposed for tracking far-field fast-moving sources using a small aperture antenna array. Initially, a spatiotemporal state space model was presented in conjunction with the concept of the extended manifold vector. Then, this model was integrated with an arrayed EKF to provide overall a powerful multi-source tracking algorithm. The performance of the proposed approach was examined using computer simulation studies under various noise levels and the results indicate high accuracy and robustness to noisy environments.

References

[1] A. Masnadi-Shirazi and B. D. Rao, "A covariance-based superpositional CPHD filter for multisource DOA tracking," *IEEE Transactions on Signal Processing*, vol. 66, no. 2, pp. 309–323, Jan. 2018.

[2] G. Wang, J. Xin, J. Wang, N. Zheng, and A. Sano, "Subspace-based twodimensional direction estimation and tracking of multiple targets," *IEEE Transactions on Aerospace and Electronic Systems*, vol. 51, no. 2, pp. 1386–1402, Apr. 2015.

[3] E. S. Baker and R. D. DeGroat, "A correlation-based subspace tracking algorithm," *IEEE Transactions on Signal Processing*, vol. 46, no. 11, pp. 3112–3116, Nov. 1998.

[4] H. Yan and H. Fan, "Signal-Selective DOA Tracking for Wideband Cyclostationary Sources," *IEEE Transactions on Signal Processing*, vol. 55, no. 5, pp. 2007–2015, May 2007.

[5] C. R. Rao, C. R. Sastry, and B. Zhou, "Tracking the direction of arrival of multiple moving targets," *IEEE Transactions on Signal Processing*, vol. 42, pp. 1133-1144, May 1994.

[6] C. R. Sastry, E.W. Kamen, and M. Simaan, "An efficient algorithm for tracking the angles of arrival of moving targets," *IEEE Transactions on Signal Processing*, vol. 39, no. 1, pp. 242–246, Jan. 1991.

[7] C. K. Sword, M. Simaan, and E. W. Kamen, "Multiple target angle tracking using sensor array outputs," *IEEE Transactions on Aerospace and Electronic Systems*, vol. 26, no. 2, pp. 367–373, Mar. 1990.

[8] S. B. Park, C. S. Ryu, and K. K. Lee, "Multiple target angle tracking algorithm using predicted angles," *IEEE Transactions on Aerospace and Electronic Systems*, vol. 30, no. 2, pp. 643–648, Apr. 1994.

[9] Y. Zhou, P. C. Yip, and H. Leung, "Tracking the direction-of-arrival of multiple moving targets by passive arrays: Algorithm," *IEEE Transactions on Signal Processing*, vol. 47, no. 10, pp. 2655–2666, Oct. 1999.

[10] M. Orton and W. Fitzgerald, "A Bayesian approach to tracking multiple targets using sensor arrays and particle filters," *IEEE Transactions on Signal Processing*, vol. 50, no. 2, pp. 216–223, Feb. 2002.

[11] A. Manikas and M. Sethi, "Joint multipath delay and direction tracking for CDMA array systems," *Vehicular Technology Conference*, May 2002, pp. 175-179

[12] B. Balakumar, S. Shahbazpanahi, and T. Kirubarajan, "Joint MIMO channel tracking and symbol decoding using Kalman filtering," *IEEE Transactions on Signal Processing*, vol. 55, no. 12, pp. 5873 –5879, Dec. 2007.

[13] V. Cevher, J. McClellan, "Sensor array calibration via tracking with the extended Kalman filter," *IEEE International Conference on Acoustics, Speech, and Signal Processing*, May 2001, pp. 2817-2820

[14] Y. Kamil and A. Manikas, "Multisource Spatiotemporal Tracking Using Sparse Large Aperture Arrays," *IEEE Transactions on Aerospace and Electronic Systems*, vol. 53, no. 2, pp. 837 - 853, Feb. 2017.

[15] A. Manikas, V. Sridhar and Y. I. Kmail, "Array of sensors: A spatiotemporal-state-space model for target trajectory tracking," *IEEE Sensor Array and Multichannel Signal Processing Workshop*, July 2016, pp. 1-5